RSC Advances

PAPER

View Article Online
View Journal | View Issue

Cite this: *RSC Adv.*, 2020, **10**, 19254

The effects of Stone–Wales defects on the thermal properties of bilayer armchair graphene nanoribbons

Xingli Zhang, *[ac] Jinglan Zhang[a] and Ming Yang*[bc]

We investigate the influence of Stone–Wales (S–W) defects on the thermal properties of bilayer graphene nanoribbons (BGNRs) with armchair edges by nonequilibrium molecular dynamics simulations (NEMD). It is shown that an increasing number of S–W defects leads to a significant decrease of the thermal conductivity of BGNRs at room temperature. Moreover, the AA-stacked BGNRs have significantly higher thermal conductivity than that of the AB-stacked BGNRs for all S–W defect numbers. In the temperature range of 300–700 K, the S–W defects always have a weaker effect on heat transfer of AB-stacked BGNRs than AA-stacked BGNRs, which is closely related to their weaker anharmonic effects induced by structure defects. In addition, the simulation results are further explained by performing an analysis of phonon spectrum properties and phonon vibrational modes.

Received 17th March 2020
Accepted 5th May 2020

DOI: 10.1039/d0ra02480e

rsc.li/rsc-advances

Introduction

Graphene nanoribbons have outstanding thermal transport properties due to their honeycomb lattice structure consisting of sp^2 bonds, and have attracted immense interest in high performance electronic applications.[1–3] Compared with monolayer graphene nanoribbons, bilayer graphene nanoribbons (BGNRs) have a relatively lower thermal conductivity because of the grain boundaries in each layer and weak coupling between layers. However, experimentally, the thermal conductivity of BGNRs still reaches 2800 W m^{-1} K^{-1}, much larger than that of most other thermally conductive materials.[4,5] In addition, BGNRs are more advantageous in their sensitivity to external perturbation and tunability with a perpendicular electric field. These factors raise the exciting prospect of using BGNRs as promising materials in nanotechnology.[6,7] It is well known that synthesis, processing and integration of BGNRs could result in various defects, such as point vacancies, Stone–Wales and impurities.[8] These structure defects strongly influence the heat transfer performance of BGNRs inevitably. The effects caused by defects are not only disadvantages, on the contrary, they provide a route to manipulate the thermal conductivity of BGNRs to achieve new functionalities by intentionally introducing these defects.

Stone–Wales (S–W) defects are the class of topological defects in nature, consisting of two pairs of pentagons and heptagons rings, which are the result of a rotation of the C–C bond by 90°. The S–W defects are one of the most common defects in graphene, which can be observed and characterized in graphene by high resolution transmission electron microscopy.[9,10] Some investigations about the effect of S–W defects on thermal transport properties of graphene have also been reported. Krasavin *et al.*[11] used the phonon Boltzmann transport equation (BTE) to calculate the thermal conductivity of graphene nanoribbons (GNRs) with the S–W defects scatterings taken into account, and a pronounced decrease of the thermal conductivity due to S–W defects is found at low temperatures; Yeo *et al.*[12] found that the presence of SW defects can decrease the thermal conductivity of GNRs in the temperature range 100–600 K by more than 80% as defect densities are increased to 10% coverage; Ebrahimi *et al.*[13] using molecular dynamics (MD) simulations, explored the influence of the concentrations of the S–W defects on the thermal conductivity of zigzag and armchair GNRs. However, almost the previous studies have been devoted to exploring effects of S–W defects on thermal properties of monolayer graphene, and the investigations on BGNRs are relatively lacking.

In this paper we study and compare the effect of S–W defects on the thermal transport properties of BGNRs with two stacking orders, AB-stacked and AA-stacked. Furthermore, using MD simulations, the modulations on defects number and temperature dependence of thermal conductivity are investigated. By analyzing of the phonon properties of the atoms, we reveal the underlying physical mechanism of thermal transport in the BGNRs.

[a]*College of Mechanical and Electrical Engineering, Northeast Forestry University, Harbin 150040, China. E-mail: zhang-xingli@nefu.edu.cn*

[b]*Institute of Engineering Thermophysics, Chinese Academy of Sciences, Beijing 100190, China. E-mail: yangming@iet.cn*

[c]*Department of Mechanical Engineering, University of Colorado, Boulder, CO, 80309, USA*

Model and methodology

We perform the non-equilibrium molecular dynamics simulation (NEMD) with the LAMMPS code. The AIREBO potential is used to describe the interactions of the carbon atoms within same layers, and the Lennard-Jones potential is used to describe the van der Waals interactions for carbon atoms between different layers. This study used samples consisting of 1600 atoms and the S–W defects are randomly introduced by a 90° rotation of two adjacent atoms, as shown in Fig. 1, thus the increasing number of S–W defects in each layer are achieved by the rotation of 1, 2, 3 and 4 pairs of atoms. The S–W defects number of two layers are same and the defects must not be connected with each other in the same layer.

Fig. 2 shows the simulation model used in the present study. The adiabatic wall is fixed at each end of BGNRs to prevent atoms escaping from the system, and the fixed boundary condition is applied. The hot and cold reservoirs regions are used to create a temperature gradient in the system by controlling the energy given or taken from these regions. We divide the simulation system (excluding the adiabatic zones at the two ends) along the heat flux direction into 42 equal segments. The instantaneous local temperature in each segment is evaluated from the kinetic energy of the atoms within it using the formula $K_E = (3/2) \times K_B \times T$, where K_B is Boltzmann constant. While the simulation temperature is below the Debye temperature (322 K), quantum corrections are conducted to calculate the temperatures.

The time step for the simulation is set as 0.5 fs. The simulations consist of two stages: the first stage is to ensure the whole system reach a steady state in a constant-temperature ensemble (NVT) with a coupling time of 10^6 MD steps; the second stage is to keep the energy conserved in a constant-energy ensemble (NVE) with a coupling time of 2×10^6 MD steps. Based on the Fourier law of conduction, the thermal conductivity is given as:

$$\lambda = \frac{\Delta E}{A\tau(\partial T/\partial x)} \quad (1)$$

where, τ is the simulation step time; A is the cross-sectional area; $(\partial T/\partial x)$ is the temperature gradient; ΔE is the energy transported in every unit time. The thermal conductivity results presented here are averaged over three independent simulations with different initial S–W defect distributions, and the error bars are obtained from the standard deviation of the three values.

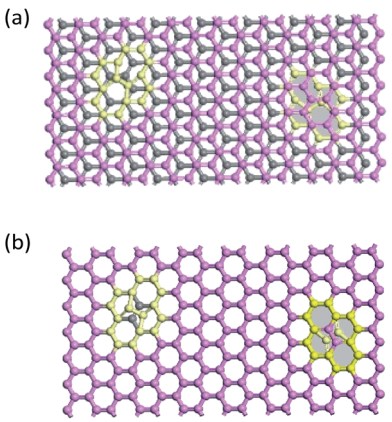

Fig. 1 Illustration of BGNRs containing S–W defects configuration (a) AB stacking type; (b) AA stacking type.

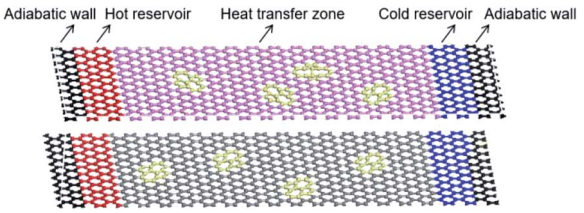

Fig. 2 The NEMD simulation model of BGNRs configuration.

Results and discussion

Fig. 3 shows the thermal conductivities of AB-stacked and AA-stacked BGNRs with different numbers of S–W defects. As it can be seen, the increasing defect number from 0 to 4 induces remarkable changes to the thermal transport properties of BGNRs. For example, containing four S–W defect in each layer leads to 38% and 46% reduction of thermal conductivity, corresponding to AB and AA-stacked BGNRs, respectively. Such result expresses the same changing trend compared with the results in ref. 14 and 15 which measured the thermal conductivity of monolayer GNRs doping S–W defects by computational method. It should be noted that the thermal conductivities obtained in this study are clearly smaller than these of previous works due to the different potentials used and size effects.[16–18] Additionally, as can be observed, the thermal conductivity of AA-stacked BGNRs is much greater than the AB-stacked BGNRs for samples of the same number of S–W defects. The theoretical calculations from Berber *et al.*[19] suggested that the thermal conductivity of multilayer graphene was reduced comparing to monolayer graphene because of the presence of interlayer coupling, so the difference of thermal conductivity between two type of BGNRs may be attributed to this factor. It has been also reported that the top layer of AB-stacked BGNRs has more wrinkles than its bottom layer, which could result in a strong suppression of thermal transport between two layers due to the significant phonon mismatch.[15] Therefore, the thermal conductivity of AB-stacked BGNRs is much lower than that of AA-stacked case.

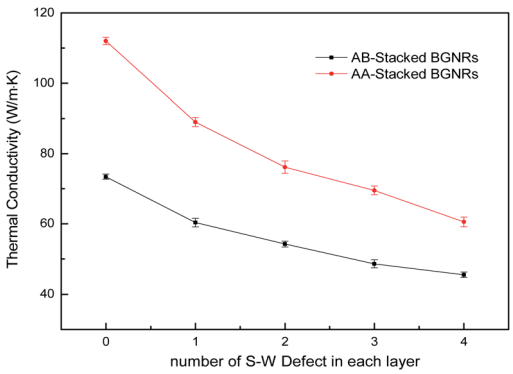

Fig. 3 The number of S–W defects dependence of thermal conductivity in BGNRs at 300 K.

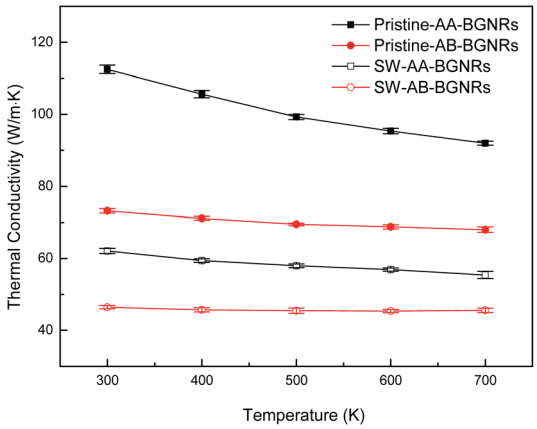

Fig. 4 The temperature dependence of thermal conductivity in BGNRs.

Fig. 4 presents the thermal conductivity of BGNRs with S–W defects as a function of the temperature from 300 to 700 K. The thermal property of BGNRs with S–W defects has less dependency on temperature compared with the pristine system, which shows obvious reduction of thermal conductivity with the increasing temperature due to the effect of phonon umklapp scattering.[20] Moreover, the thermal conductivity of AB-stacked BGNRs is more insensitive to the temperature changes than that of AA-stacked style. The structural disorder effects of thermal conductivity for low dimensional materials were studied in ref. 21 and 22 based on modal localization analysis and Allen-Feldman approach, and it was confirmed that the suppression of thermal conductivity due to structure defects was shown to be mild. This originates from the presence of low frequency vibrational modes, which could maintain a well-defined polarization and help preserve the thermal conductivity in the presence of disorder. Additionally, the AB-stacked BGNRs have more stable structure than AA-stacked BGNRs under natural condition, which may reduce more sensitivity of the phonon coupling and phonon umklapp scattering due to the increased temperature. The tendency of the variation of thermal conductivities in our simulation is in good agreement with the temperature dependence on the thermal conductivity of the monolayer graphene nanoribbons with S–W defect.[23]

In order to find the thermal transport mechanism of this simulation, the phonon frequency spectrum of BGNRs that represents vibrational energy of carbon atoms per unit frequency is investigated as shown in Fig. 5. The phonon spectrum function $G(\omega)$ is determined by calculating the Fourier transform of the velocity autocorrelation function.[24] Fig. 5 indicates that the peaks of $G(\omega)$ at frequencies around 50 THz are damped out and shift towards low frequency when the AA-stacked and AB-stacked BGNRs contain 4 S–W defects, suggesting that the S–W defects might decrease the phonon mean free path due to high collision of the low energy phonons. It is also revealed that the phonon scattering is the main factor in reducing thermal conductivity in multilayer graphene structures.[25] Comparing Fig. 5(a) and (b), it can be seen that the peaks of AA-stacked BGNRs decrease more largely than the AB-

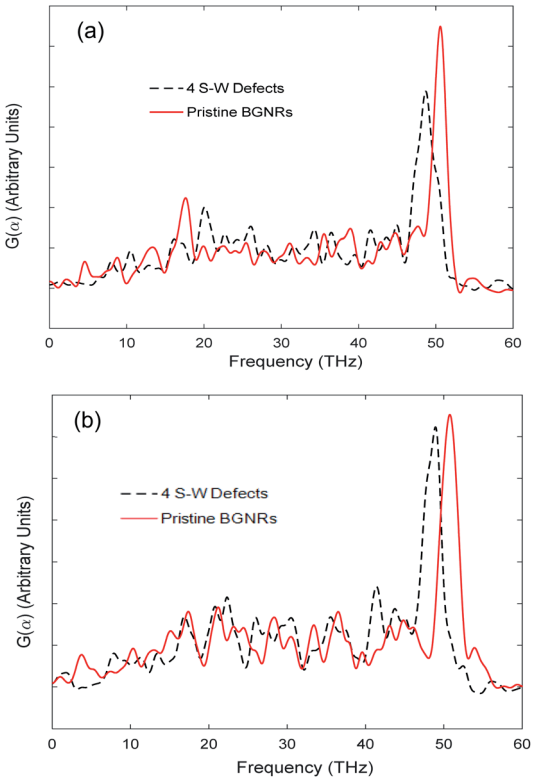

Fig. 5 The phonon spectra of BGNRs with different number of S–W defects at 300 K (a) AA-stacked; (b) AB-stacked.

stacked case, which is consistent with the reduction results of thermal conductivity. It means that S–W defects lead to a greater impact on AA-stacked BGNRs under same condition.

We also analyze the phonon vibrational modes through the calculation of phonon participation ratio to reveal the thermal transport essence of BGNRs doping S–W defects. The participation ratio is used to describe the fraction of atoms participating in a particular phonon mode, which is defined as:[26,27]

$$P_\lambda^{-1} = N\sum_i^N \left(\sum_\alpha \varepsilon_{i\alpha,\lambda}^* \varepsilon_{i\alpha,\lambda}\right)^2 \quad (2)$$

where, i sums over all the atoms studied; α is a Cartesian direction and sums over x, y, and z; $\varepsilon_{i\alpha,\lambda}$ is the vibrational eigenvector component of the mode λ at the α direction of the i_{th} atom; N is the total number of atoms. Here, $P = 1$ means that all atoms take part in a specific phonon mode and the phonon mode is completely delocalized; $P < 1$ means there are partial atoms participating in the motion and phonon mode is localized, thus the phonon modes with smaller P value can't transport thermal energy sufficiently.

We plot the phonon participation ratio of AA-stacked and AB-stacked BGNRs in Fig. 6. It is clear that the S–W defects make a large reduction in the participation ratio of BGNRs compared with the pristine case, indicating the existence of more localized modes due to structure defects. For S–W defects structure, the numerous localizations induce inelastic phonon scatterings, which could increase the total number of possible scattering

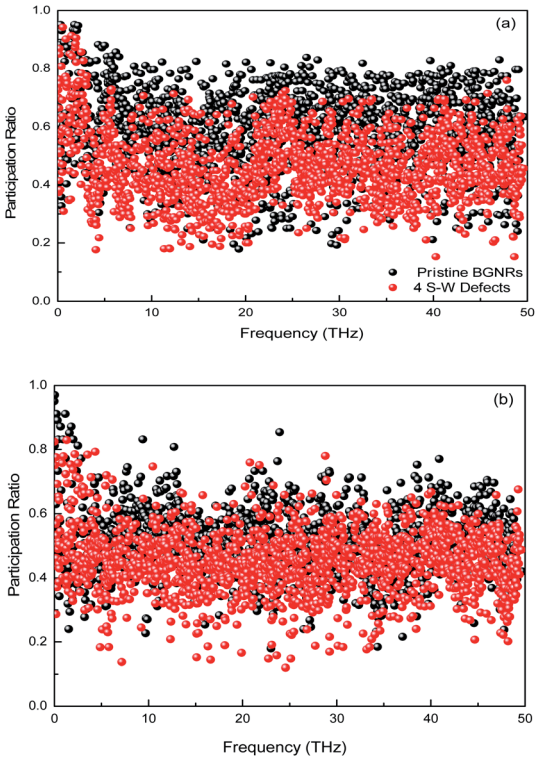

Fig. 6 The phonon participation ratio of BGNRs with different number of S–W defects at 300 K (a) AA-stacked; (b) AB-stacked.

outcomes. Consequently, this reduces the effective capability of the BGNRs to transmit thermal energy across the S–W defects.[28] Additionally, it can be observed that the overall phonon participation ratio of AB-stacked BGNRs is less than that of AA-stacked BGNRs, which indicates that the AB-stacked ordering may enhance phonon localizations in BGNRs compared with AA-stacked case.

Conclusions

In summary, we have performed NEMD method to study the effect of S–W defects on thermal transport properties of BGNRs. It is found that the S–W defects could effectively influence the thermal conductivity of the AB-stacked and AA-stacked BGNRs. For difference numbers of S–W defects and temperatures, the thermal conductivity of AA-stacked BGNs is much higher than that of AB-stacked one due to the weaker interlayer coupling. In addition, the thermal conductivity of AB-stacked BGNRs has less of a dependence on temperature. The phonon frequency spectrum results suggest that the S–W defects might decrease the phonon mean free path due to high collision of the low energy phonons in BGNRs. Moreover, the phonon vibrational modes analysis reveals that the S–W defects also cause the increase of phonon localizations in BGNRs, which lead to the reduction of thermal conductivity.

Conflicts of interest

There are no conflicts to declare.

Acknowledgements

The work has been supported by the National Natural Science Foundation of China (grant no. 51706039 and 51606192).

Notes and references

1 J. Hu, X. Ruan and Y. P. Chen, *Nano Lett.*, 2015, **9**, 2730–2735.
2 A. A. Balandin, S. Ghosh, W. Z. Bao, I. Calizo, D. Teweldebrhan and F. Miao, *Nano Lett.*, 2208, **8**, 902–907.
3 S. J. Mahdizadeh and E. K. Goharshadi, *J. Nanopart. Res.*, 2014, **16**, 2553.
4 Y. Tang, J. Li, Xi. Wu, Q. Liu and Y. Liu, *Appl. Surf. Sci.*, 2016, **362**, 86–92.
5 W. R. Zhong, M. P. Zhang and B. Q. Ai, *Appl. Phys. Lett.*, 2011, **98**, 113107.
6 S. Q. Hu, J. Chen, N. Yang and B. W. Li, *Carbon*, 2017, **116**, 139–144.
7 T. Lehmann, D. A. Ryndyk and G. Cuniberti, *Phys. Rev. B: Condens. Matter Mater. Phys.*, 2013, **88**, 125420.
8 J. Kotakoski, F. R. Eder and J. C. Meyer, *Phys. Rev. B: Condens. Matter Mater. Phys.*, 2014, **89**, 201406.
9 S. P. Wang, J. G. Guo and L. J. Zhou, *Phys. E*, 2013, **48**, 29–35.
10 H. Malekpour, P. Ramnani, S. Srinivasan, G. Balasubramanian, D. L. Nika, A. Mulchandani, R. K. Lakee and A. A. Balandin, *Nanoscale*, 2016, **8**, 14608–14616.
11 S. E. Krasavin and V. A. Osipov, *J. Phys.: Condens. Matter*, 2015, **27**, 425302.
12 Y. J. Jie, L. Zishun and N. T. Yong, *Nanotechnology*, 2012, **23**, 385702.
13 S. Ebrahimi and M. Azizi, *Mol. Simulat.*, 2017, 1366654.
14 D. L. Feng, Y. H. Feng, Y. Chen, W. Li and X. X. Zhang, *Chin. Phys. B*, 2013, **22**, 016501.
15 Y. Liu, H. Yang, N. Liao and P. Yang, *RSC Adv.*, 2014, **4**, 54474.
16 Z. X. Guo, D. Zhang and X. G. Gong, *Appl. Phys. Lett.*, 2009, **95**, 163130.
17 W. W. Cai, A. L. Moore, Y. W. Zhu, X. S. Li, S. S. Chen and L. Shi, *Nano Lett.*, 2010, **10**, 1645–1651.
18 X. Nie, L. Zhao, S. Deng, Y. Zhang and Z. Du, *Int. J. Heat Mass Tran.*, 2019, **137**, 161–173.
19 S. Berber, Y. K. Kwon and D. Tomanek, *Phys. Rev. Lett.*, 2000, **84**, 46130–46136.
20 H. Zhan, Y. Zhang, J. M. Bell and Y. Gu, *J. Phys. Chem. C*, 2015, **119**, 1748–1752.
21 T. Zhu and E. Ertekin, *Nano Lett.*, 2016, **16**, 4763–4772.
22 T. Zhu and E. Ertekin, *Phys. Rev. B*, 2016, **93**, 155414.
23 T. Y. Ng, J. J. Yeo and Z. S. Liu, *Carbon*, 2012, **50**, 4887–4893.
24 S. K. Chien, Y. T. Yang and C. K. Chens, *Phys. Lett. A*, 2010, **374**, 4885.
25 S. Ghosh, W. Bao, D. L. Nika, S. Subrina, E. P. Pokatilov and C. N. Lau, *Nat. Mater.*, 2010, **9**, 555–558.
26 X. Zhang, M. Hu, K. P. Giapis and D. Poulikakos, *J. Heat Tran.*, 2012, **134**, 102402.
27 Y. Wang, A. K. Vallabhaneni, B. Qiu and X. Ruan, *Nanoscale Microscale Thermophys. Eng.*, 2014, **18**, 155–182.
28 C. Shao, Q. Rong, N. Li and H. Bao, *Phys. Rev. B*, 2018, **98**, 155418.